forests

MDPI

Article

Research on the End-Milling Surface Quality of *Paulownia* Based on Response Surface Model in Terms of Force and Chip Morphology

Jinxin Wang [1], Zhanwen Wu [1], Feng Zhang [1], Chaojun Song [1], Wei Hu [1], Zhaolong Zhu [2,3], Xiaolei Guo [1] and Pingxiang Cao [1,*]

[1] College of Materials Science and Engineering, Nanjing Forestry University, Nanjing 210037, China; jackiewang@njfu.edu.cn (J.W.); wuzhanwen@njfu.edu.cn (Z.W.); njfuzhangfn@njfu.edu.cn (F.Z.)
[2] College of Furnishings and Industrial Design, Nanjing Forestry University, Nanjing 210037, China
[3] Co-Innovation Center of Efficient Processing and Utilization of Forest Resources, Nanjing Forestry University, Nanjing 210037, China
* Correspondence: njfucpx@163.com

Abstract: To investigate the impact of different milling parameters on milling forces, chip morphology, and machined surface quality during the *Paulownia* milling process, we conducted experiments using cemented carbide single-tooth shank milling cutters. Additionally, we established a response surface model (RSM) to analyze milling surface quality. The key findings are as follows: milling forces along the parallel and tangential axes decrease with an increased tool rake angle and spindle's rotational frequency, but they exhibit a positive correlation with milling depth. The effect of spindle's rotational frequency on the milling force along the lateral axis differs due to the complex fiber characteristics of *Paulownia*. As milling depth decreases, chip morphology transitions from a block structure to a sheet structure, eventually becoming fragmented with shallow milling. Higher spindle's rotational frequency and tool rake angle lead to a more fragmented direction in *Paulownia* chip morphology, while machined surface quality improves. Notably, under specific conditions, a striped chip morphology significantly enhances machined surface quality compared to similar milling parameters. The established RSM for machined *Paulownia* surface roughness is reliable and holds reference value for inhibiting surface damage in *Paulownia* machining.

Keywords: *Paulownia*; chip morphology; milling parameters; surface damage suppression; RSM

Citation: Wang, J.; Wu, Z.; Zhang, F.; Song, C.; Hu, W.; Zhu, Z.; Guo, X.; Cao, P. Research on the End-Milling Surface Quality of *Paulownia* Based on Response Surface Model in Terms of Force and Chip Morphology. *Forests* **2024**, *15*, 325. https://doi.org/10.3390/f15020325

Academic Editor: Anuj Kumar

Received: 18 December 2023
Revised: 30 January 2024
Accepted: 5 February 2024
Published: 8 February 2024

1. Introduction

The genus *Paulownia* is originated in China, it has ability to grow large sizes in a very short time [1,2]. As a raw material widespread used to make boards and decorative materials, such as particleboard, plywood, house siding, window shutters, etc. Due to its straight texture, uniform structure, and easy processing, *Paulownia* has been widely consumed in the field of furniture manufacturing [3]. Meanwhile, *Paulownia* furniture has been highly praised in China and Japan. However, some *Paulownia* wood density and hardness is too low to avoid plastic deformation and defects during cutting, such as tear, burr and pits in the cutting process, which will have a great impact on the quality of products and subsequent processing [4].

Milling is the most commonly used cutting process in the wood cutting and furniture industry [5,6]. Some studies have shown that, in wood material processing, cutting tools and cutting parameters have a decisive effect on the surface quality [7,8]. No matter whether one is milling soft or solid wood, it has been found that the cutting angle, feed speed, wood fiber orientation angle, and milling depth that are used have significant influences on the cutting force, chip formation, and surface quality [9,10]. As a typical

soft wood, *Paulownia* requires fundamental investigation into its machinability due to the currently lack of information surrounding it in the literature.

The most basic movement in milling is the action of force: the tool cuts into the wood's surface; then, the chips separate to form a machined surface. In this process, there are a series of actions, such as shear force, friction force, workpiece rebound force, and so on; finally, these synthesize into the milling force [11,12]. Therefore, the importance of studying the cutting force is self-evident. Marchal et al. [13] presented a case evidencing the strong relationship between the cutting force and surface roughness. Furthermore, a higher cutting force is likely to introduce the severe vibrations in the tools, leading to severe defects on the machined surface. In addition, the orientation angle of wood fibers plays a significant role in relation to the cutting force component in the machining of wood [14].

Milling movement is accompanied by chip removal; different milling parameters will produce different shapes of chip, indicating that the milling mechanism is presently variable. Study of the relationship between chip shape and surface quality is helpful in determining the chip formation mechanism and thus enabling practitioners to set appropriate machining parameters [15–17].

In general, although much of the literature has made great efforts in researching the wood milling process, there is little research on the machining of *Paulownia*. This work presents the following differences from previously published studies: (1) a fundamental investigation into the effect of milling parameters on milling performance, including milling force, chip morphology, and the surface quality of *Paulownia*; (2) an analysis of the mechanisms of chip formation during milling of *Paulownia* under different milling parameters; (3) an initial regression model of surface quality in the milling of *Paulownia* is established.

The objective of this work is to study the machinability of *Paulownia* under different milling parameters in terms of the milling force, chip morphology, and surface quality. The designed full-factor experiments were carried out to reveal the relationship between milling parameters and resulting characteristics. This work provides new knowledge of *Paulownia* milling, which will serve to guide high-efficiency and high-quality *Paulownia* machining.

2. Materials and Methods

2.1. Materials

As shown in Figure 1c, the milling workpiece is five-year-old *Paulownia* from Shandong, China. This was cut into a size of 120 × 80 × 15 mm. The red number on the surface of specimen is the workpiece number during the experiment. The length direction for the wood fiber's axial direction was consistent; this ensures that the milling process is one of nearly longitudinal milling. It is important to avoid defects, such as knots and cracks on the surface, to enable processing. This was ensured to prevent any wood defects from interfering with the test results. The mean value of the equilibrium moisture content was tested by assessing 10 random specimens under controlled conditions of constant temperature and humidity in an incubator (20 °C and 65% RH, respectively). *Paulownia* timber properties are shown in Table 1.

Table 1. Physical and mechanical properties of *Paulownia*.

Workpiece	Density (g/cm^3)	Moisture Content (%)
Paulownia	0.285	11.91

The woodworking tool used in the test was a cemented, carbide, single-tooth shank milling cutter (Figure 1b), produced by Leitz Co., Ltd., Oberkochen, Germany. The measurement from the cutter tooth to the rotary shaft is 30 mm, the length of the cutter tooth is 30 mm, and the maximum milling depth is 1.5 mm. The wedge angle of the cutter is fixed

at 45°. The density is 14.8 g/cm^3. The bending strength and hardness are 2100 N/cm^2 and 89 HRC, respectively. The varied parameters of this test are shown in Table 2, based on the literature [18,19].

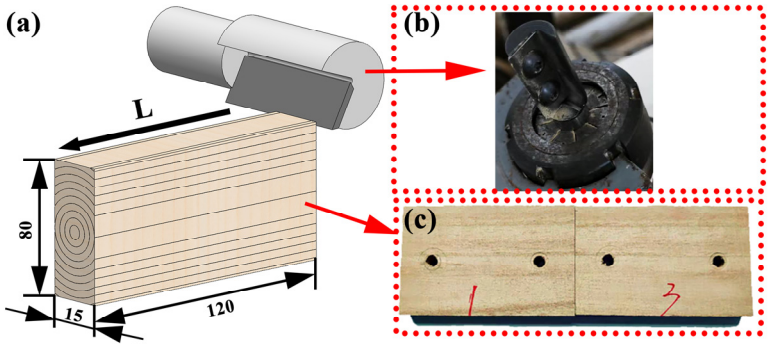

Figure 1. *Paulownia* milling diagram: (**a**) milling diagram; (**b**) milling tool; (**c**) *Paulownia* workpiece.

Table 2. The input parameters of the test.

No.	Rake Angle γ (°)	Rotation Frequency n (r/min)	Milling Depth h (mm)
1	2	6000	0.5
2	6	8000	1.0
3	10	10,000	1.5

2.2. Experiment Design

As shown in Figure 2, the *Paulownia* workpiece was positioned on a five-axis CNC machining center (MGK01, Nanxing Machinery Co., Ltd., Hong Kong, China, Figure 2a). The milling test of the *Paulownia* workpiece was carried out by changing the spindle's rotational frequency, the milling depth, and tool rake angle; a fixed feed speed was used. The milling parameters were selected according to the pre-experiment, actual factory processing parameters, and the limitations of the machining tool. During the milling test, the milling force data were transmitted to the signal amplifier in real time through the Kistler dynamometer (Kistler 9257B, Kistler Group, Winterthur, Switzerland, Figure 2b); the milling force data were obtained in three directions (F_x, F_y and F_z). The surface roughness after the test was measured by the roughness measuring instrument (DSX510, Olympus, Co., Ltd., Osaka-fu, Japan, Figure 2c). Each set of data was measured five times and averaged. The morphology of the chips was measured by a micrometer (ZW H1600, China Micro Semiconductor (Shenzhen) Co., Ltd., Shenzhen, China, Figure 2d). Our design for the milling parameters is presented in Table 2. One milling tool was used for each test to control the rounding of the cutting edge.

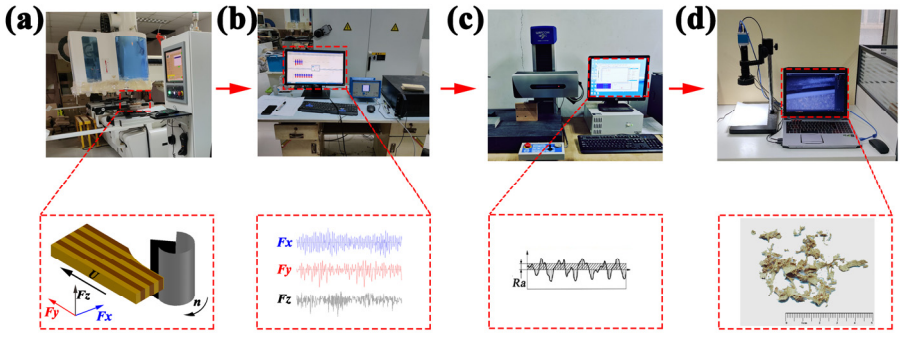

Figure 2. Test instruments: (**a**) machine tool; (**b**) dynamometer; (**c**) surface roughness measuring instrument; (**d**) micrometer.

Chip thickness is the vertical distance between the milling trajectories of two adjacent cutter teeth. As shown in Figure 3, the chip thickness varies with the position of the cutter teeth in the workpiece during milling. When the cutter teeth make contact with the workpiece, the chip thickness $a = 0$. At the moment when the cutter teeth leave the workpiece, the maximum chip thickness is a_{max}. Taking the contact arc as the average calculation point, the average chip thickness, a_{av}, is calculated using Equation (1) [20]:

$$a_{av} = U_Z \cdot \sqrt{\frac{h}{D}} = \frac{1000 \cdot U}{n \cdot Z} \cdot \sqrt{\frac{h}{D}}, \quad (1)$$

where U_Z (mm/Z) is the feed per tooth, U (m/min) is the feed speed, and the feed speed is fixed at 5 m/min. n (r/min) is the spindle's rotational frequency; Z is the number of teeth participating in milling; h (mm) is the milling depth; D (mm) is the maximum milling diameter of the tool (the tool used in this paper has a diameter of 30 mm).

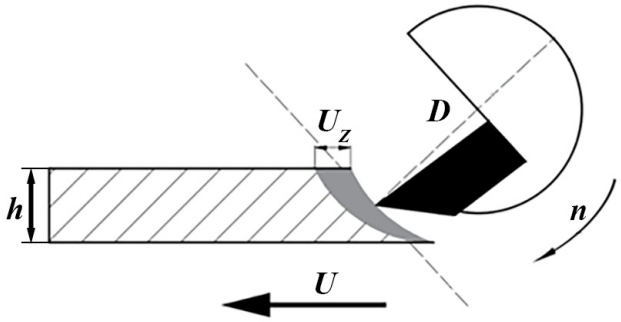

Figure 3. Schematic diagram of chip formation.

The response surface method (RSM) is one of the most widely used mathematical models. In this study, the Box–Benhnken design method was used to design the three input parameters at three levels via Design-Expert (Version 13) [21]. The response surface regression model is shown in Equation (2) [22].

$$Y = \beta_0 + \sum_{i=1}^{m} \beta_i x_i + \sum_{ij}^{m} \beta_{ij} x_i x_j + \sum_{i=1}^{m} \beta_{ii} x_i^2, \quad (2)$$

where Y is the response (Ra), X is the experimental factors (e.g., spindle's rotational frequency n, and depth of milling h, rake angle γ), β_0 is the free term, β_1, β_2, …, β_i are coefficients for linear terms, β_{11}, β_{22}, …, β_{ii} are coefficients for quadratic terms, and β_{12}, β_{13}, …, $\beta_{i-1,j}$ are coefficients for interacting terms.

3. Results and Discussion

3.1. Milling Force

In *Paulownia* milling, the milling parameters will have a decisive influence on the milling force. The milling force can reflect the machining state of the machine tool to a certain extent and have a profound impact on the milling quality. The experiment results are shown in Table 3.

3.1.1. The Influence of Milling Parameters on F_x

As shown in Figure 4, by enumerating the individual data of each milling force, we were able to analyze the influence of the change of milling parameters on the milling force, F_x, parallel to the X axis. F_x was negatively correlated with tool rake angle and spindle's rotational frequency, and positively correlated with milling depth. With the increase in the tool rake angle, the contact area between tool rake face and workpiece (as shown in Figure 4) decreases, and the friction between them decreases. When the spindle's

rotational frequency increases, the amount of milling per tooth decreases (as shown in Equation (2)), and is reduced in the milling process; here, the cutting edge's load is small, and the vibration is reduced. Therefore, the whole machining process is more stable, which makes the F_x lower [23]. As the milling depth, h, increases, the amount of milling per tooth and the impact load increase, resulting in an increase in F_x.

Table 3. Experimental results and standard deviations.

Ex. No.	γ (°)	n (r/min)	h (mm)	F_x	Std.	F_y	Std.	F_z	Std.	Ra	Std.
1	2	6000	0.5	96.41	4.98	177.60	2.15	46.81	7.56	5.53	1.65
2	2	8000	0.5	82.53	6.73	148.10	3.79	58.20	5.16	5.46	1.26
3	2	10,000	0.5	75.26	8.46	122.80	6.80	62.38	1.26	3.95	0.27
4	2	6000	1.0	106.20	5.65	196.30	3.52	53.91	8.57	5.65	1.17
5	2	8000	1.0	100.90	7.27	168.90	5.16	64.29	6.57	5.08	2.28
6	2	10,000	1.0	90.97	8.36	136.30	9.68	71.20	2.99	4.99	0.26
7	2	6000	1.5	110.70	5.09	210.20	1.15	70.05	9.57	7.65	1.84
8	2	8000	1.5	103.40	6.49	184.70	6.17	84.55	8.56	6.59	0.68
9	2	10,000	1.5	98.63	8.96	158.00	8.65	96.57	7.68	6.32	1.63
10	6	6000	0.5	91.32	4.98	149.00	4.68	32.55	5.26	5.33	1.27
11	6	8000	0.5	73.23	5.27	132.40	6.17	39.26	7.59	4.86	0.27
12	6	10,000	0.5	64.18	8.61	98.60	7.61	42.28	3.40	4.46	1.13
13	6	6000	1.0	101.50	6.90	167.00	3.68	48.66	8.56	5.39	1.27
14	6	8000	1.0	88.21	7.53	155.30	3.94	58.43	1.27	5.21	5.25
15	6	10,000	1.0	83.37	9.41	127.00	4.90	64.58	4.60	4.72	1.61
16	6	6000	1.5	114.90	3.53	172.00	2.11	58.53	3.95	5.98	0.40
17	6	8000	1.5	94.89	5.44	158.70	5.17	64.88	5.30	5.56	1.29
18	6	10,000	1.5	81.15	7.18	146.60	8.29	70.08	8.60	5.32	2.38
19	10	6000	0.5	80.58	4.89	138.60	4.17	29.48	9.27	5.21	0.59
20	10	8000	0.5	72.80	6.62	122.50	4.99	38.85	2.98	4.69	1.23
21	10	10,000	0.5	67.06	8.48	93.20	6.17	49.58	5.27	4.48	0.67
22	10	6000	1.0	86.32	2.49	118.20	1.18	43.67	4.30	5.38	1.00
23	10	8000	1.0	73.61	4.19	107.50	5.29	48.21	7.86	4.95	1.27
24	10	10,000	1.0	61.87	7.14	103.90	8.27	55.94	7.68	4.72	0.21
25	10	6000	1.5	95.15	5.47	132.70	4.12	46.48	1.38	5.90	2.24
26	10	8000	1.5	85.42	8.18	118.20	5.99	61.48	5.29	5.23	1.68
27	10	10,000	1.5	68.74	8.84	102.70	8.84	71.01	2.68	4.98	0.68

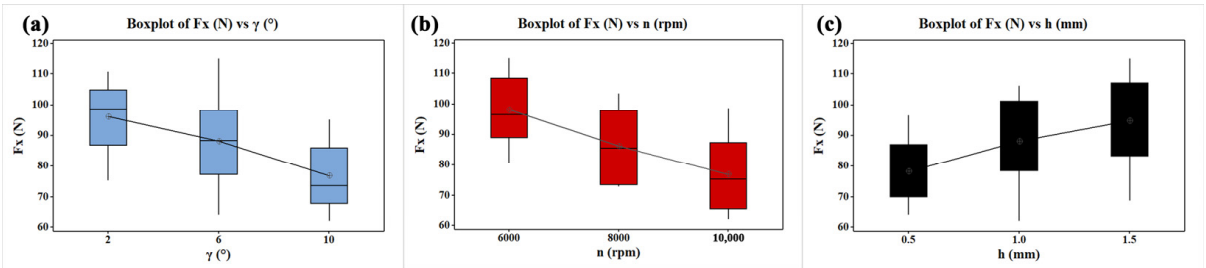

Figure 4. The influence of milling parameters on F_x: (**a**) rake angle; (**b**) spindle rotational frequency; (**c**) milling depth.

3.1.2. The Influence of Milling Parameters on F_y

Figure 5 shows the influence of each milling parameter on the milling force, F_y, parallel to the Y-axis. Compared with F_x, the influence regularity of the milling parameters on F_y is same. It is important to note that, in the numerical F_y, the whole is greater than F_x. This is because the milling force, F_x, parallel to the X-axis, mainly acts on milling wood fibers, and wood is relatively soft compared to cemented carbide tools. Simultaneously, because the wedge angle of woodworking tools is small and the cutting edge is sharp, the milling force

value is smaller. However, the milling force, F_y, parallel to the Y-axis, separates the chips from the workpiece surface in the milling process to form the machined surface. At the same time, it overcomes the large-area friction between the chips and the rake face, and finally overcomes the elastic restoring force of the workpiece. This leads to the F_y being larger in value [24,25].

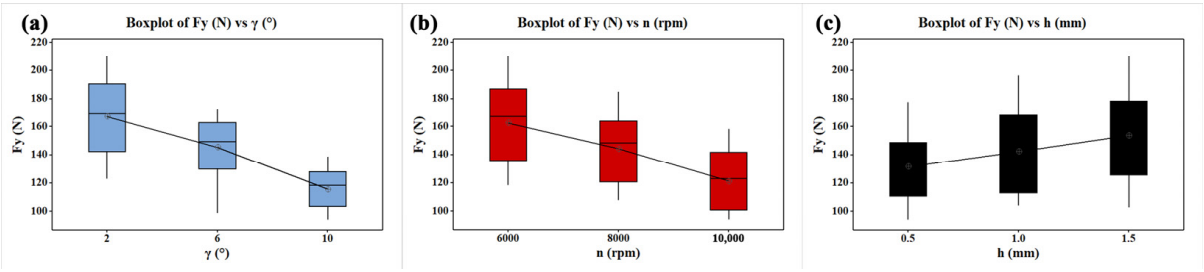

Figure 5. The influence of milling parameters on F_y: (**a**) rake angle; (**b**) spindle rotational frequency; (**c**) milling depth.

3.1.3. The Influence of Milling Parameters on F_z

Figure 6 shows the influence of milling parameters on the milling force, F_z, parallel to the Z-axis. Compared with F_x and F_y, the influence of the tool rake angle and the milling depth on F_z is consistent. The main difference is that, with the increase in the spindle's rotational frequency, F_z presents with an increasing trend. For longitudinal milling, the feed direction is parallel to the fiber direction; however, because of the complexity of the structure of *Paulownia*, in the process of the cutter's removal of the chips, it is bound to cause a tearing force that is perpendicular to the fibers' direction, resulting in an increase in F_z [26].

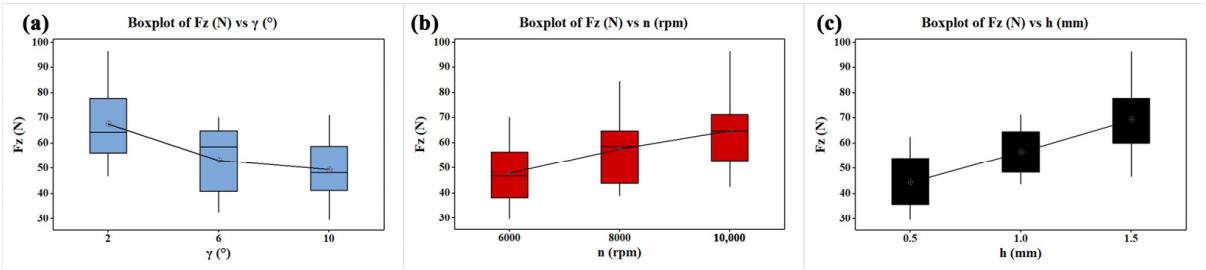

Figure 6. The influence of milling parameters on F_z: (**a**) rake angle; (**b**) spindle rotational frequency; (**c**) milling depth.

We used a mean response analysis to obtain a ranking of the influence degrees of each cutting parameter on the milling forces, F_x, F_y and F_z, in the three directions. The rank value was sorted in descending order based on the size of delta. The results are listed in Table 4. The ranking of the influence degree of each milling parameter on the milling forces in the three different directions is different. Among them, the spindle's rotational frequency has the greatest influence on F_x; this is mainly attributable to the face that the change in the milling force of each tooth significantly affects F_x. The most significant influence on F_y is the tool rake angle, which shows that the friction between the chips and the rake face significantly affects F_y. The milling depth has the greatest influence on F_z; it increases obviously with the increase in milling depth.

Table 4. Means response table of milling forces.

	F_x			F_y			F_z		
Level	γ (°)	n (r/min)	h (mm)	γ (°)	n (r/min)	h (mm)	γ (°)	n (r/min)	h (mm)
1	96.11	98.12	78.15	167	162.4	131.4	67.55	47.79	44.38
2	88.08	86.11	88.11	145.2	144	142.3	53.25	57.57	56.54
3	76.84	76.8	94.78	115.3	121	153.8	49.41	64.85	69.29
Delta	19.27	21.32	16.62	51.7	41.4	22.3	18.14	17.05	24.92
Rank	**2**	**1**	**3**	**1**	**2**	**3**	**2**	**3**	**1**

3.2. Chip Morphology

3.2.1. The Influence of Spindle's rotational frequency on Chip Morphology

As shown in Figure 7, the chip morphology changes with the spindle's rotational frequency when the tool rake angle is γ = 2° and the milling depth h = 0.5 mm. As the spindle's rotational frequency increases, there is a transition in the chip characteristics from large, curled chips to smaller chips, accompanied by a notable decrease in chip integrity and adhesion. The relationship between the spindle's rotational frequency and the feed per tooth, as described by Equation (1), is inversely proportional. For a given feed speed, the corresponding feeds per tooth at the three different spindle rotational frequencies are 0.833, 0.625, and 0.500 mm/Z. Since the cutter is a single-tooth shank milling cutter, the feed per tooth is equivalent to the feed per revolution. This implies that, with higher spindle rotational frequency, the tool cuts fewer wood fibers per revolution, resulting in smaller chip morphology and reduced bonding between chips [27].

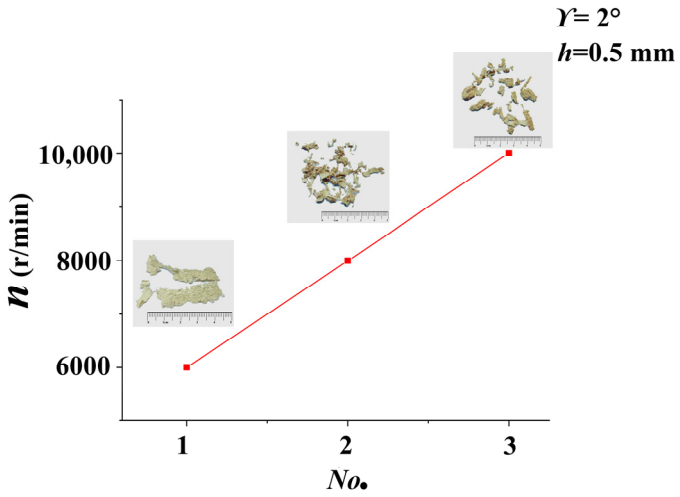

Figure 7. The influence of n on chip morphology.

3.2.2. The Influence of Rake Angle on Chip Morphology

Figure 8 shows the change in the chip morphology with the tool rake angle when the spindle's rotational frequency is n = 8000 r/min and the milling depth is h = 0.5 mm. With the increase in the tool rake angle, the chip morphology changes from flaky to granular. The rake angle of the tool affects the deformation of the milling layer. The larger the rake angle, the smaller the deformation of the milling layer. This is evident from the morphology of the chips. The extension along the feed direction is lower and the feed amount per tooth is the same. Under these circumstances, the chips will be scattered and broken [28].

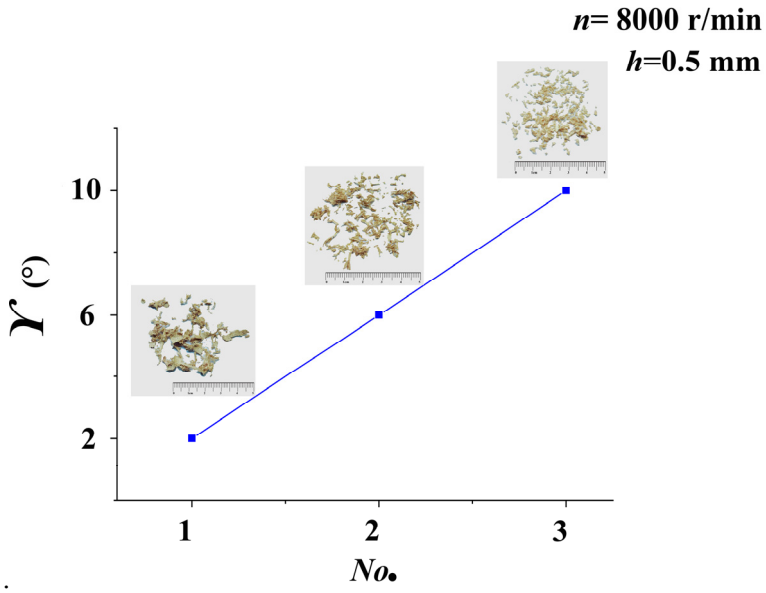

Figure 8. The influence of γ on chip morphology.

3.2.3. The Influence of Milling Width on Chip Morphology

Table 5 presents five distinct chip morphologies, along with their corresponding milling parameters and machined surface roughness. The average absolute value, a_{av}, was calculated using Equation (1). As the milling thickness diminishes, a noticeable transformation in chip shape occurs. They transform from top block chips to middle flake chips. These progress to strip chips, characterized by excellent integrity, and ultimately to progress scattered chips. This indicates a pronounced effect of milling thickness on chip morphology. Concurrently, it is observed that, with decreasing milling thickness, there is a corresponding decrease in the roughness of the machined surface [29].

Table 5. The morphology of the chip and the corresponding milling parameters and surface roughness.

No.	γ (°)	h (mm)	n (r/min)	a_{av} (mm)	Ra (μm)	Chips Morphology
1	2	1.5	6000	0.2406	7.65	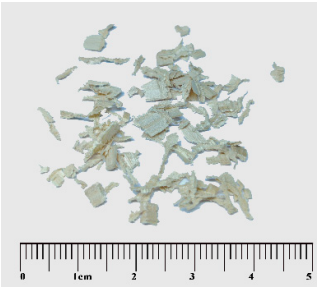
2	2	1.5	8000	0.1804	6.59	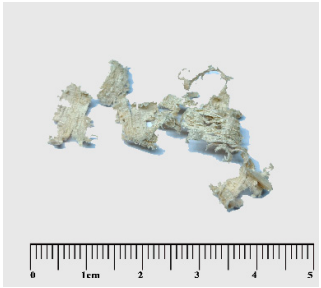

Table 5. *Cont.*

No.	γ (°)	h (mm)	n (r/min)	a_{av} (mm)	Ra (μm)	Chips Morphology
3	2	1.0	8000	0.1473	5.08	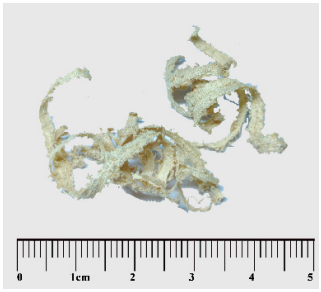
4	2	0.5	6000	0.1389	5.53	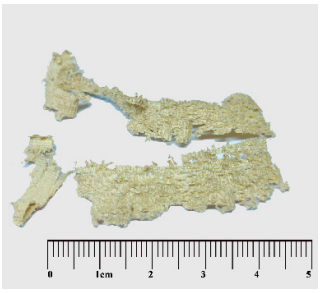
5	2	1.0	10,000	0.1178	4.99	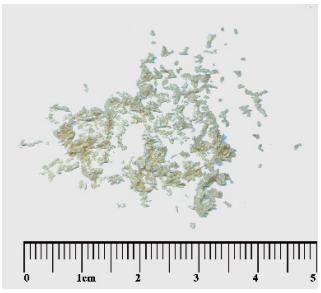

Of particular importance is the observation that, under the milling conditions of the third group, strip chips with exceptional integrity appear. Surprisingly, the machined surface of the workpiece exhibits lower surface roughness even when compared to the fourth group, with a smaller milling thickness. This highlights a significant relationship between chip morphology and milling surface quality, emphasizing the importance of studying chip morphology in understanding and optimizing the machining process [30].

3.3. Surface Quality

3.3.1. Machined Surface Damage

As depicted in Figure 9, the predominant surface damage observed post *Paulownia* milling consists of burrs and tears. During the wood milling process, using a milling edge to generate chips, wood fibers undergo a shear force, resulting in a machined surface. Due to the inherent elastoplastic nature of wood, chip removal is not entirely smooth, leading to tearing and bonding of the wood fibers. This tearing extends upward, forming burrs, and downward, forming tears. Table 5 indicates that appropriately chosen milling parameters significantly reduce surface roughness when producing strip chips, suggesting that there is a potential to mitigate *Paulownia* milling surface damage and enhance machined quality by selecting suitable milling parameters. The establishment of a model correlating cutting parameters with *Paulownia* milling surface quality holds substantial reference significance [11].

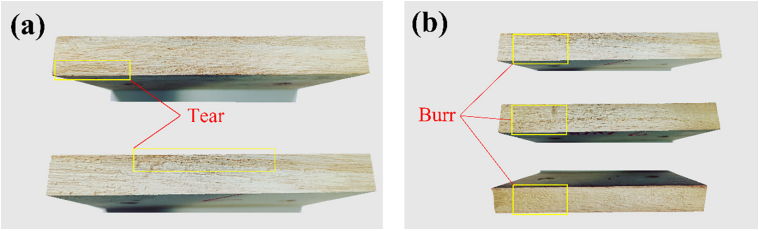

Figure 9. Processed defects of *Paulownia* workpiece: (**a**) tear; (**b**) burr.

3.3.2. The RSM Model of *Ra*

According to Equation (2) and the data in Table 3, a response surface model of the *Paulownia* milling surface roughness is established, as shown in Equation (3). As shown in Table 6, the R-square of the model is 0.9117, which is close to 1, indicating that the model is successful. Meanwhile, Adeq precision measures the signal/noise ratio. A ratio greater than 4 is desirable. The ratio of the model is 11.258, indicating an adequate signal. This model can be used to navigate the design space.

$$\begin{aligned} Ra = \quad & 5.22 - 0.3575n + 0.3988h - 0.3338\gamma + 0.05nh \\ & -0.1475h\gamma - 0.1269n^2 + 0.1806h^2 + 0.0907\gamma^2 \end{aligned} \tag{3}$$

Table 6. Fit statistic of *Ra* model.

Model	Standard Deviation	Mean	C.V.%	R^2	Adeq Precision
Ra	0.2205	5.29	4.17	0.9117	11.2577

Figure 10 shows a 3D surface map and contour map of the influence of milling parameters on *Ra*. The surface roughness decreased with the increase in the spindle's rotational frequency and the tool rake angle and will increase with an increase in milling depth. The coefficients of the spindle's rotational frequency, the tool rake angle, and the milling depth were all more than 0.3, showing a significant influence on surface roughness. The main order of their influence on surface roughness is $h > n > \gamma$. The square terms of each factor and the interaction of the two factors are low.

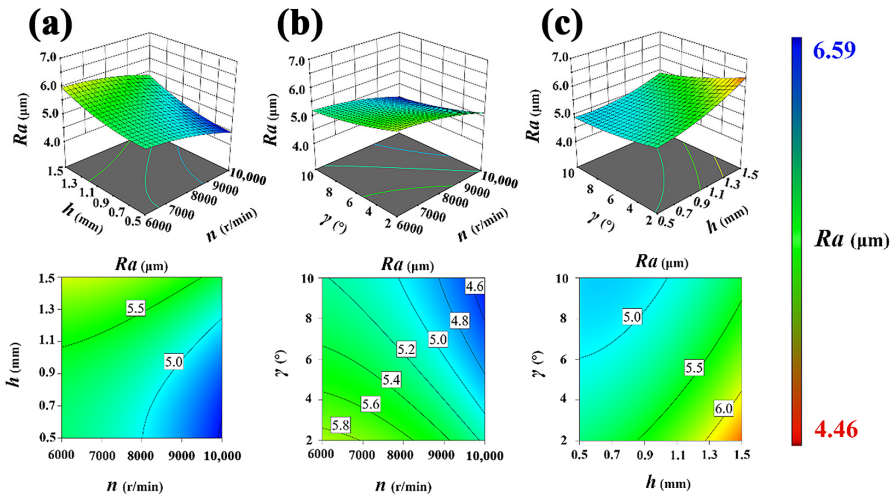

Figure 10. Three-dimensional surface map and contour map of the influence of milling parameters on *Ra*: (**a**) milling depth and the spindle's rotational frequency; (**b**) tool rake angle and the spindle's rotational frequency; (**c**) tool rake angle and the spindle's rotational frequency.

4. Conclusions

In this paper, the milling force, chip morphology, and surface quality in the milling process of *Paulownia* were studied, and the potential rules among them were explored. The main conclusions are as follows:

(1) Increasing the tool rake angle and the spindle's rotational frequency leads to a decrease in milling forces along the parallel and tangential axes. However, milling forces increase with the milling depth. The spindle's rotational frequency has a unique impact on milling forces along the lateral axis due to the complex fiber characteristics of *Paulownia*.

(2) Higher spindle rotational frequency and rake angle result in *Paulownia* chips developing in a more fragmented direction. Despite the fragmented chip morphology, the machined quality improves with increased spindle rotational frequency and rake angle. Under specific conditions, a striped chip formation significantly enhances the quality of the machined surface compared to similar milling parameters.

(3) The response surface methodology (RSM) for *Paulownia* milling surface roughness is considered to be more credible. This established RSM has a reference value for research on reducing damage to the *Paulownia* milling surface.

Author Contributions: Conceptualization, J.W. and Z.W.; methodology, Z.W. and C.S.; software, F.Z.; validation, Z.Z., X.G. and P.C.; formal analysis, J.W.; investigation, W.H.; resources, X.G.; data curation, Z.W. and C.S.; writing—original draft preparation, J.W.; writing—review and editing, Z.W. and Z.Z.; visualization, X.G.; supervision, P.C.; project administration, P.C.; funding acquisition, X.G. and Z.Z. All authors have read and agreed to the published version of the manuscript.

Funding: This research was supported by the National Natural Science Foundation of China [grant. number 31971594]; the Natural Science Foundation of the Jiangsu Higher Education Institutions of China [21KJB220009]; the Self-Made Experimental and Teaching Instruments of Nanjing Forestry University in 2021 [nlzzyq202101]; the project from Technology Innovation Alliance of Wood/Bamboo Industry [TIAWBI2021-08]; the International Cooperation Joint Laboratory for Production, Education, Research and Application of Ecological Health Care on Home Furnishing.

Data Availability Statement: The raw data supporting the conclusions of this article will be made available by the authors on request.

Conflicts of Interest: The authors declare no conflicts of interest.

References

1. Akyildiz, M.H.; Kol, H.S. Some technological properties and uses of paulownia (*Paulownia tomentosa* Steud.) wood. *J. Environ. Biol.* **2010**, *31*, 351–355.
2. Jakubowski, M. Cultivation Potential and Uses of *Paulownia* Wood: A Review. *Forests* **2022**, *13*, 668. [CrossRef]
3. Kaygin, B.; Gunduz, G.; Aydemir, D. Some physical properties of heat-treated paulownia (*Paulownia elongata*) wood. *Dry. Technol.* **2009**, *27*, 89–93. [CrossRef]
4. Rencoret, J.; Marques, G.; Gutiérrez, A.; Nieto, L.; Jiménez-Barbero, J.; Martínez, Á.T.; del Río, J.C. Isolation and structural characterization of the milled-wood lignin from *Paulownia fortunei* wood. *Ind. Crops Prod.* **2009**, *30*, 137–143. [CrossRef]
5. Gochev, Z. Examination the process of longitudinal solid wood profile milling. Part II: Influence of the revolution frequency and feed rate on the roughness of the treated surfaces. *Innov. Woodwork. Eng. Des.* **2014**, *1*, 48–54.
6. Isleyan, Ü.K.; Karamanoglu, M. The Influence of Machining Parameters on Surface Roughness of MDF in Milling Operation. *Bioresources* **2019**, *14*, 3266–3277. [CrossRef]
7. Wei, W.H.; Cong, R.; Xue, T.M.; Abraham, A.D.; Yang, C.Y. Surface Roughness and Chip Morphology of Wood-plastic Composites Manufactured via High-speed Milling. *Bioresources* **2021**, *16*, 5733–5745. [CrossRef]
8. Eriksen, E. The influence of surface roughness on the mechanical strength properties of machined short-fibre-reinforced thermoplastics. *Compos. Sci. Technol.* **2000**, *60*, 107–113. [CrossRef]
9. Curti, R.; Marcon, B.; Denaud, L.; Togni, M.; Furferi, R.; Goli, G. Generalized cutting force model for peripheral milling of wood, based on the effect of density, uncut chip cross section, grain orientation and tool helix angle. *Eur. J. Wood Wood Prod.* **2021**, *79*, 667–678. [CrossRef]

10. Ibrisevic, A.; Obucina, M.; Hajdarevic, S.; Mihulja, G.; Kuzman, M.K.; Busuladzic, I. Effects of Cutting Parameters and Grain Direction on Surface Quality of Three Wood Species Obtained by CNC Milling. In *Bulletin of the Transilvania University of Brasov*; Series II: Forestry, Wood Industry, Agricultural Food Engineering; Transilvania University Press: Lexington, KY, USA, 2023; pp. 127–140.
11. Darmawan, W.; Azhari, M.; Rahayu, I.S.; Nandika, D.; Nishio, S. The chips generated during up-milling and down-milling of pine wood by helical router bits. *J. Indian Acad. Wood Sci.* **2018**, *15*, 172–180. [CrossRef]
12. Li, B.; Wang, X.; Hu, Y.; Li, C. Analytical prediction of cutting forces in orthogonal cutting using unequal division shear-zone model. *Int. J. Adv. Manuf. Technol.* **2011**, *54*, 431–443. [CrossRef]
13. Marchal, R.; Mothe, F.; Denaud, L.E.; Thibaut, B.; Bleron, L. Cutting forces in wood machining—Basics and applications in industrial processes. A review COST Action E35 2004–2008: Wood machining—Micromechanics and fracture. *Holzforschung* **2009**, *63*, 157–167. [CrossRef]
14. Cyra, G.; Tanaka, C. The effects of wood-fiber directions on acoustic emission in routing. *Wood Sci. Technol.* **2000**, *34*, 237–252. [CrossRef]
15. Liu, C.; Wang, G.; Dargusch, M.S. Modelling, simulation and experimental investigation of cutting forces during helical milling operations. *Int. J. Adv. Manuf. Technol.* **2012**, *63*, 839–850. [CrossRef]
16. Caceres, C.B.; Uliana, L.; Hernandez, R.E. Orthogonal cutting study of wood and knots of white spruce. *Wood Fiber Sci.* **2018**, *50*, 55–65. [CrossRef]
17. Cao, P.X.; Zhu, Z.L.; Buck, D.; Guo, X.L.; Ekevad, M.; Wang, X. Effect of rake angle on cutting performance during machining of stone-plastic composite material with polycrystalline diamond cutters. *J. Mech. Sci. Technol.* **2019**, *33*, 351–356. [CrossRef]
18. Xu, W.Y.; Wu, Z.W.; Lu, W.; Yu, Y.Y.; Wang, J.X.; Zhu, Z.L.; Wang, X.D. Investigation on Cutting Power of Wood-Plastic Composite Using Response Surface Methodology. *Forests* **2022**, *13*, 1397. [CrossRef]
19. Zhu, Z.L.; Buck, D.; Wang, J.X.; Wu, Z.W.; Xu, W.; Guo, X.L. Machinability of Different Wood-Plastic Composites during Peripheral Milling. *Materials* **2022**, *15*, 1303. [CrossRef]
20. Guo, X.L.; Wang, J.X.; Buck, D.; Zhu, Z.L.; Ekevad, M. Cutting forces and cutting quality in the up-milling of solid wood using ceramic cutting tools. *Int. J. Adv. Manuf. Technol.* **2021**, *114*, 1575–1584. [CrossRef]
21. Box, G.E.P.; Wilson, K.B. On the experimental attainment of optimum conditions. In *Breakthroughs in Statistics: Methodology and Distribution*; Springer: New York, NY, USA, 1992; pp. 270–310. [CrossRef]
22. Zhu, Z.L.; Buck, D.; Guo, X.L.; Xiong, X.Q.; Xu, W.; Cao, P.X. Energy Efficiency Optimization for Machining of Wood Plastic Composite. *Machines* **2022**, *10*, 104. [CrossRef]
23. Li, R.; Yang, F.; Wang, X. Modeling and Predicting the Machined Surface Roughness and Milling Power in Scot's Pine Helical Milling Process. *Machines* **2022**, *10*, 331. [CrossRef]
24. Li, R.; Yao, Q.; Xu, W.; Li, J.; Wang, X. Study of cutting power and power efficiency during straight-tooth cylindrical milling process of particle boards. *Materials* **2022**, *15*, 879. [CrossRef]
25. Wei, H.; Guo, X.; Zhu, Z.; Cao, P.; Wang, B.; Ekevad, M. Analysis of Cutting Performance in High Density Fiberboard Milling by Ceramic Cutting Tools. *Wood Res.* **2018**, *63*, 455–466.
26. Hu, W.; Wan, H.; Guan, H. Size Effect on the Elastic Mechanical Properties of Beech and Its Application in Finite Element Analysis of Wood Structures. *Forests* **2019**, *10*, 783. [CrossRef]
27. Nalbant, M.; Altin, A.; Gökkaya, H. The effect of cutting speed and cutting tool geometry on machinability properties of nickel-base Inconel 718 super alloys. *Mater. Des.* **2007**, *28*, 1334–1338. [CrossRef]
28. Thasthakeer, A.T.; Farid, A.A.; Seng, C.T.; Namazi, H. Analysis of the Correlation between Fractal Structure of Cutting Force Signal and Surface Roughness of Machined Workpiece in End Milling Operation. *Fractals* **2019**, *27*, 1950013. [CrossRef]
29. Shi, W.; Ma, Y.; Yang, C.; Jiang, B.; Li, Z. Evaluation of a regression prediction model for surface roughness of wood–polyethylene composite (WPC). *Surf. Rev. Lett.* **2017**, *24*, 1850033. [CrossRef]
30. Kayahan, E.; Oktem, H.; Hacizade, F.; Nasibov, H.; Gundogdu, O. Measurement of surface roughness of metals using binary speckle image analysis. *Tribol. Int.* **2010**, *43*, 307–311. [CrossRef]